XLVI CILAMCE
VITÓRIA - ES - BRAZIL - 2025
XLVI IBERO-LATIN AMERICAN CONGRESS ON COMPUTATIONAL METHODS IN ENGENEERING

MODELING AND SIMULATION OF PULL-OUT OF FLEXIBLE LAZY-WAVE RISERS

Luis C. N. Filho[1], Luana A. M. Brock[1], Leonardo G. Ribeiro[1], Evandro Parente Jr[1], Antônio M. C. de Melo[1], Marcelo S. M. Júnior[1], Elias S. Barroso[1]

[1]*Departamento de Engenharia Estrutural e Construção Civil.*
Universidade Federal do Ceará, Campus do Pici, Bloco 733, 60440-900, Fortaleza, Ceará, Brasil.
filho.lcf@alu.ufc.br, luanaandreza@alu.ufc.br, leonardoribeiro@alu.ufc.br , evandro@ufc.br, macario@ufc.br, marcelomedeiros@ufc.br, elias.barroso@ufc.br

Abstract. The decommissioning of offshore structures is a challenge due to the numerous factors influencing the decision-making process regarding the methodology to be adopted. Activity planning involves a multidisciplinary study that considers regulatory, logistical, economic, environmental, and operational issues. One of the main stages is the pull-out, which consists of disconnecting and retrieving the flexible pipes. Consequently, there is a constant search for alternatives to optimize this activity. A simple and economical alternative is the surface cutting of the riser followed by its free fall to the seabed. Assessing the technical feasibility of this alternative requires computational simulations to determine the geometry and internal forces during the fall. Thus, this work aims to develop a computational model able to simulate the surface cutting of a flexible lazy-wave riser. The studied parameters include mesh discretization, the time increment of the integration algorithm, and the effect of the drag coefficient. Initially, the static configuration of the riser was obtained. Subsequently, the surface cutting of the structure was simulated, followed by a study of the riser's configuration during the fall, the envelopes of velocity, effective tension, and curvature radius, which are all essential for analysis of the operation.

Keywords: Flexible risers, Lazy-wave, Decommissioning, Pull-out, Nonlinear analysis.

1 Introduction

The decommissioning of offshore Stationary Production Units (SPUs) has become a relevant topic in the oil and gas industry, as many assets approach the end of their operational life. Decommissioning can be defined as the set of activities primarily associated with the permanent shutdown of facilities and the proper disposal of materials, waste, and residues [1]. Many activities are included in the decommissioning process, where the pull-out of flexible risers is a critical step. This involves disconnecting the risers connected to the SPU, and their subsequent disposal.

In a decommissioning project, a multidisciplinary study is conducted to support decision-making, as the pull-out operation is influenced by regulatory, logistical, economic, environmental, and operational factors [2]. In Brazil, these operations are commonly performed by pulling out starting either at the connection with the FPSO or at the seabed, requiring prior planning for equipment mobilization and SPU preparation due to the installation of winches and auxiliary structures. This often results in complex, high-cost operations with significant associated risks.

Given this, it is necessary to understand the structural behavior of flexible risers during the pull-out operation. Special attention must be paid to the line integrity to avoid logistical issues and environmental damage. According to Philip et al. [3], the decommissioning program aims to provide the best alternative considering the challenges of each production unit. Among the alternatives, cutting the riser near the platform-connected end is seen as a simpler and more cost-effective option. Due to the logistical and economic challenges of these operations, one must be able to simulate pull-out operations, in order to provide information to support decision-making.

In the literature, many studies address the decommissioning of offshore oil and gas structures. However, discussions often focus solely on regulatory and logistical processes. In practice, few works provide structural analyses that support the planning of the pull-out operation for flexible risers. Nevertheless, certain related topics can be identified as contributing to the understanding of the activities involved in riser pull-out operations. First, the pull-in process stands out as a logistically equivalent activity, as it also employs support vessels, winches, cables and divers. For rigid risers such as Steel Lazy-Wave Risers (SLWR) and Steel Catenary Risers (SCR), studies also

aim to model transfer or pre-lay operations [4–6]. These studies discuss key simulation topics such as the location of the cut, effective tension, and minimum bend radius.

Previous studies on the post-failure behavior of flexible risers and slender structures discuss the expected response following a sudden disconnection. Different authors demonstrated that the release of axial tension triggers a compression wave that propagates along the structure with a celerity that depends on material properties [7–9]. This wave may induce complex phenomena including dynamic buckling, significant out-of-plane deformations, and even the formation of small bend radii. Particular emphasis is placed on factors such as initial imperfections [8], hydrodynamic drag forces [10], and nonlinear bending stiffness [9, 11]. These factors directly influence post-cut behavior and must be carefully modeled to obtain reliable simulations.

This work aims at performing the computational simulation of the pull-out of a lazy-wave riser, focusing on the behavior of the riser after performing a cut close to the surface. The influence of key simulation parameters—such as discretization and drag coefficients—on the model response is assessed. The simulations were performed using OrcaFlex software, which is widely used for analysis of offshore structures.

This paper initially examines the time increment for defining the maximum time step (TS_{max}). Subsequently, the influence of a variable normal drag coefficient is analyzed, enabling the determination of an axial drag coefficient (C_{Da}). Following this, a parametric study of the axial drag coefficient is conducted. Finally, a convergence test is performed by increasing the discretization of the riser to study the influence of element length.

2 Modeling of pull-out of flexible risers

The pull-out simulation was performed considering the model presented in Meneses et al. [9], which studied the post-failure behavior of a lazy-wave flexible riser. The initial step involved replicating the results of the static simulation. This baseline model was designated as Md-Ref. Subsequent modifications were made to adapt the model to the decommissioning condition. The internal fluid was replaced with sea water (density $d = 1.025$ t/m^3) to represent the hydrostatic equilibrium condition during pull-out operations. This model was designated as Md-Ref-W. A stiffener and two connectors were incorporated into the model to better represent real-world applications. This complete model was designated as Md-Comp. The stiffener at the top of the riser has a length of 3.85 m, density of 1.2 t/m^3, with an external diameter varying from 1.19 m to 0.35 m. The connectors are located at riser length S = 400 m and S = 2050 m from the origin and are modeled as concentrated masses of 1.16 t each.

For the simulation of riser pull-out using OrcaFlex, the cut location must be defined. In this study, the cut is assumed to occur near the surface, at S = 10 m. In OrcaFlex, the line to be decommissioned must be modeled as two separate lines from the beginning of the analysis, allowing the disconnection to be executed appropriately. The first line is connected to the platform in one end, and connected to the other line in the other end. The other line is considered free in one end (which is however restricted by the connection to the other line, as defined before), and anchored to the riser-flow connection in the other end. The cut can be simulated by releasing the connection between the two lines. This is performed during the dynamic analysis, after 5 seconds, which are considered as a build-up.

2.1 Temporal and spatial discretization

To enhance the robustness of the analysis, an implicit dynamic algorithm with a variable time step is employed, with an appropriate maximum time step (TS_{max}) defined. In this study, the normal and axial drag coefficients are set to 1.2 and $0.01/\pi$ respectively, according to Meneses et al. [10]. Due to the complexity of the simulation, it is important to pick a small time step, which should be able to capture the displacement of the riser during the fall, as well as the behavior of the compressive wave load after the cut.

Even though the time step is allowed to vary during the simulation (some steps can be performed with a smaller time step, to allow for a more robust simulation), this variation can introduce noise to the simulation, which must be avoided. Thus, the results should be studied with caution. An initial study is conducted to determine the most suitable maximum time step for the analysis, considering the range $TS_{max} \in [0.100, 0.050, 0.010, 0.005]$.

At first, spatial discretization was defined as proposed by Ribeiro et al. [11], considering the top tension and the Euler compressive limit. Accordingly, the element length (l_e) is defined as follows:

$$l_e = \pi \sqrt{\frac{EI}{T_{top}}}, \tag{1}$$

where EI is the bending stiffness and T_{top} is the top tension. Applying this equation to the present case, based on the example described in [9], results in an element length of $l_e = 0.6$ m, considering a top tension of 1494.2

kN obtained from the static analysis. To understand how spatial discretization influences the response, tests were performed considering element length in the domain $l_e \in [0.15, 0.30, 0.60, 1.20]$.

2.2 Drag coefficient

The normal drag coefficient (C_{Dn}) can be defined is a function of the Reynolds number R_e [12, 13]. For R_e between 2×10^4 and 3×10^5, the normal drag coefficient is assigned a value of 1.2, and surface roughness may be neglected. For the axial drag coefficient (C_{Da}), values of 0.008 are indicated for smooth-surface cylinders and 0.011 for rough surfaces. In high R_e conditions, the drag coefficient becomes highly dependent on both R_e itself and surface roughness. In such cases, for the tangential direction, it is acceptable to consider $C_{Da} = 0$ [12].

During the fall of the riser, the structure is subjected to high velocities, especially right after the cut, which imply high R_e. This makes it impossible to use a fixed drag coefficient of 1.2. According to the standard literature [13, 14], the C_{Dn} for high R_e is recommended as 0.65 for smooth pipes and 1.05 for rough risers. The complete curve that relates C_{Dn} and R_e can be found in Fergestad and Løtveit [13].

For a smooth-surfaced riser under these flow conditions, $C_{Dn} = 0.65$ is considered. The relationship between C_{Dn} and C_{Da} is given by [14]:

$$C_{Da} = C_{Dn} \cdot [0.03 + 0.05 \sin(\alpha)] \cos(\alpha), \tag{2}$$

where α is the angle between the flow velocity vector and the riser's longitudinal axis. Under the assumption of upward flow, Equation 2 simplifies to $C_{Da} = 0.03\, C_{Dn}$. On OrcaFlex, this coefficient must be divided by π since the tangential force is applied over the external surface area defined by $A_t = \pi D\, l$, where D is the outer diameter and l is the segment length. This differs from regulatory formulations that adopt the force application area equal to the normal component's area $A_n = D\, l$, i.e., the projection of the external surface area. Therefore, $C_{Da} = 0.03\, C_{Dn}/\pi = 0.006$.

This study examines various drag coefficients based on values presented in the OrcaFlex manual [12] and risers guidelines [13, 14]. Initially, three different cases are compared: one considering C_{Da} = 0 and C_{Dn} = 0.65, other one with C_{Da} = 0.006 and C_{Dn} = 0.65, and finally one considering C_{Da} = 0.006 and C_{Dn} as a function of R_e, according to the curve found in Fergestad and Løtveit [13]. Then, a parametric study was performed over C_{Da}, where different C_{Da} in the domain $C_{Da} \in [0.002, 0.004, 0.006, 0.008]$ were tested.

Table 1. Static results

Model	Description	Top tension (kN)	TDP (m)
Meneses (2023)	Static configuration of the reference article	1317.3	2785
Md-Ref	Model replication	1318.2	2788
Md-Ref-W	Md-Ref model with only the internal fluid changed to water	1484.2	2673
Md-Comp	Addition of stiffener and connectors	1494.2	2669

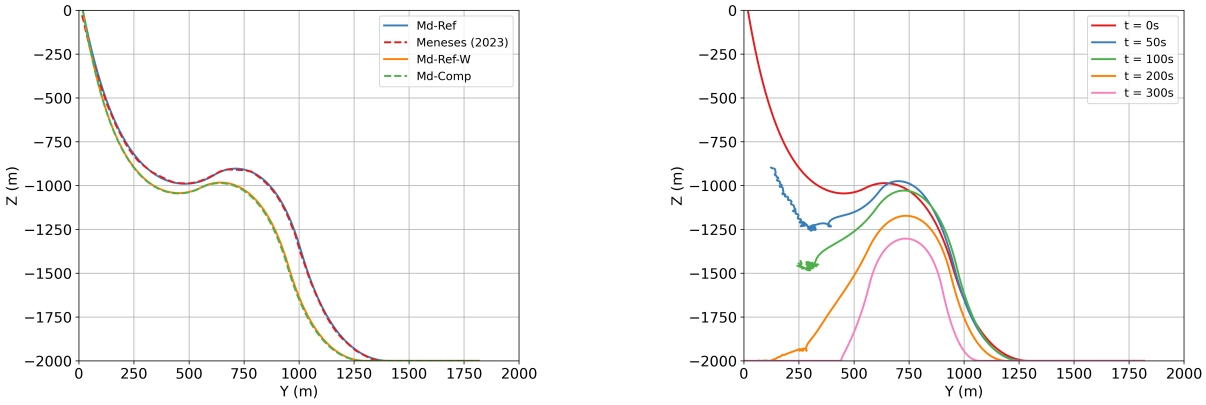
3 Results and discussion

The determination of the static configuration was the initial step of the analyses. The results from the static analyses are compared to the ones shown in the reference in Table 1, and the geometric configuration for the different models is presented in Fig. 1a. The Md-Ref model, which aimed at replicating the reference model entirely, showed a difference of only 0.07% in top tension. It also presented a very similar static configuration.

When the internal fluid was changed, Md-Ref-W, a significant difference can be noted in the riser geometry, as well as in the top tension and the touchdown point (TDP). With the addition of the stiffener and connectors (Md-Comp), a slight difference can be observed in top tension. However, the inclusion of connectors and stiffeners had minimal impact on the static response. Nevertheless, the presence of these components is relevant in the dynamic analysis, as they affect the inertia of the system. Thus, a 13% increase in effective top tension was observed in the base model (Md-Comp) when compared to the maximum static value obtained in the reference model (Md-Ref), mainly due to the internal fluid.

After performing static analysis and comparing some results with the reference, the simulation of the pull-out was performed. In this case, we considered that the riser is cut very close to the floating unit, at S = 10 m, which makes it so that the entire line starts to fall, as shown in Fig. 1b. Due to the buoyant section, there is still a segment

that does not touch the seabed. This figure also shows the complexity of the simulation, since the structure is subjected to large displacements and very high curvatures during the fall.

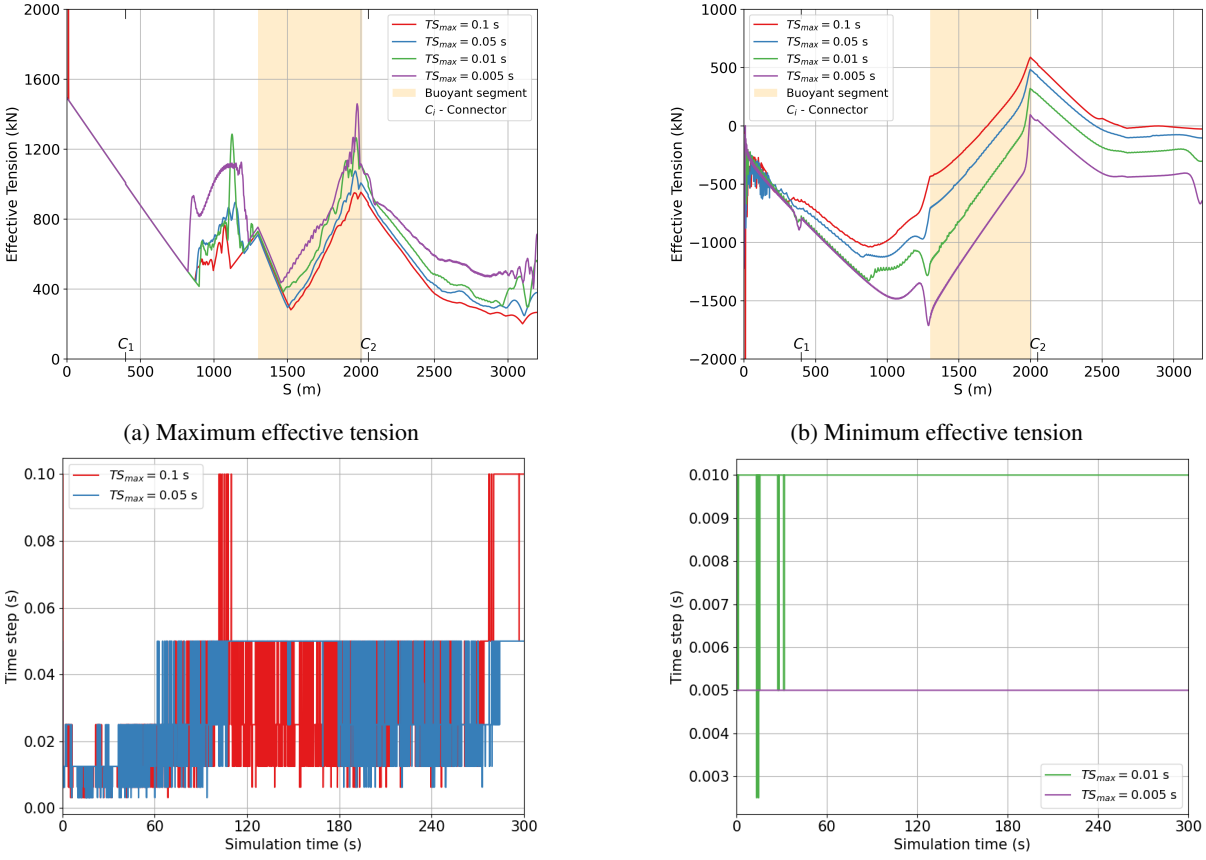


(a) Static

(b) Md-Comp in free-fall

Figure 1. Geometric configuration of the riser

To start off the parametric tests, the first parameter evaluated was the maximum time increment for the implicit algorithm adopted by OrcaFlex. Figures 2a and 2b show that TS_{max} significantly influenced the envelope of the effective tension. Regarding the minimum effective tension, it is evident that, for $TS_{max} = 0.1$ s and 0.05 s, the model exhibits convergence difficulties and numerical noise. This behavior is confirmed by analyzing the time step variation shown in Fig. 2c, as large variation in the time step adopted can be seen in these cases. A smaller variation is observed when using $TS_{max} = 0.01$ s and 0.005 s, for which no significant changes were detected, as the time step is already sufficiently small (Fig. 2d). Although $TS_{max} = 0.005$ s does not show numerical noise, convergence of the results could not yet be identified when analyzing the envelopes.



(a) Maximum effective tension

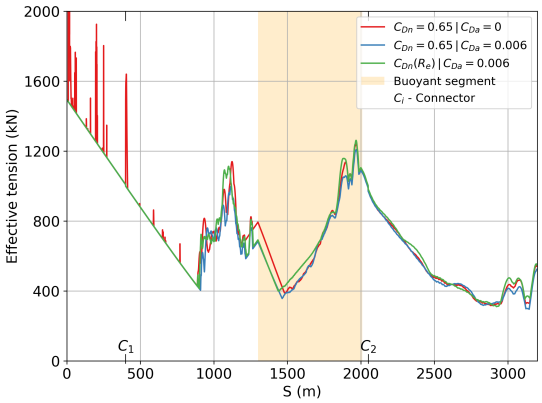
(b) Minimum effective tension

(c) $TS_{max} \in [0.1, 0.05]$

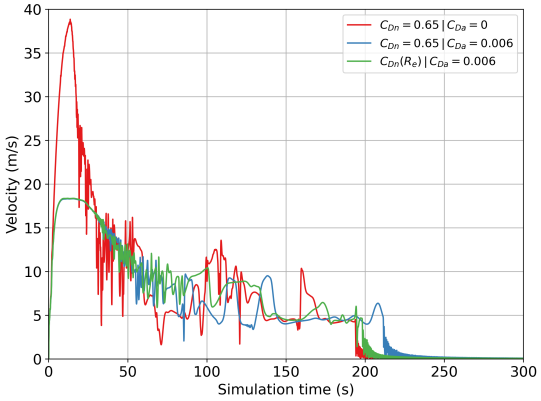
(d) $TS_{max} \in [0.01, 0.005]$

Figure 2. Study of the TS_{max}

Due to the fact that Fig. 2d shows that the model with $TS_{max} = 0.01$ s exhibits minor initial variations without numerical noise, this value was adopted for subsequent tests. After studying the effect of TS_{max}, the influence of drag coefficients in the pull-out simulation was assessed. Figure 3 shows some results found for different combinations of C_{Da} and C_{Dn}. For the case where $C_{Da} = 0$, the maximum and minimum effective tension present numerical noise and convergence difficulties, given the high time step variation throughout the simulation (see Fig. 3a). Additionally, the maximum velocity of the first connector is much higher when compared to other models with non-zero axial drag. On the other hand, the use of cases with $C_{Da} = 0.006$ for both fixed and variable C_{Dn} shows convergence for the maximum velocity and the effective tension (see Fig. 3b). This demonstrates that the axial component has a greater influence than the normal one and that disregarding C_{Da} is numerically unfeasible for the case of free-fall of flexible risers.

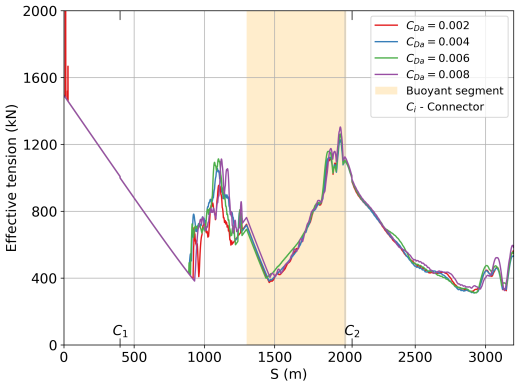


(a) Envelope of maximum effective tension.

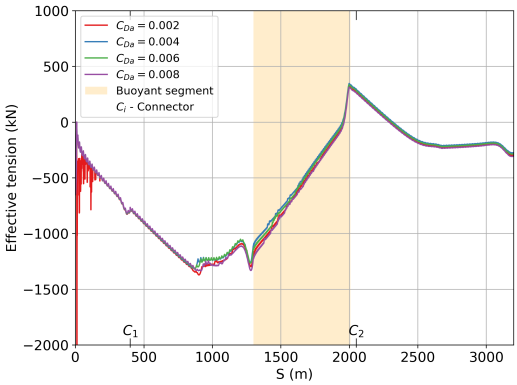


(b) Velocity of the first connector (S = 400 m)

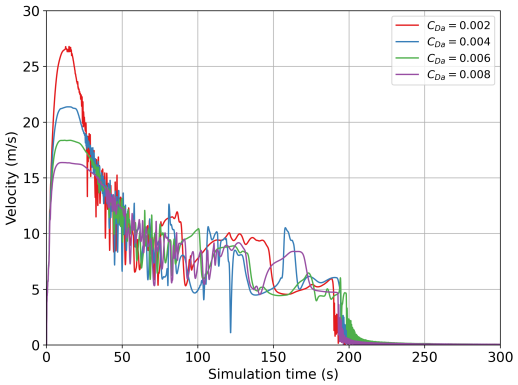
Figure 3. Results for different combinations of C_{Da} and C_{Dn}



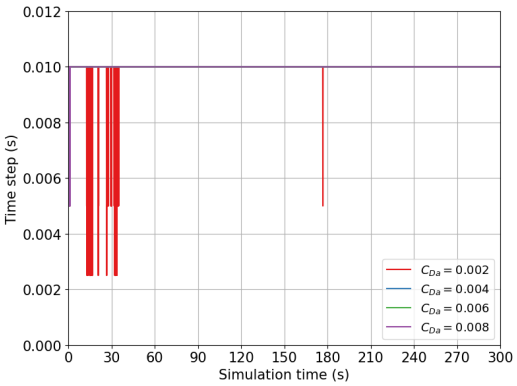
(a) Maximum effective tension envelope



(b) Minimum effective tension envelope



(c) Velocity of the first connector (S = 400m)



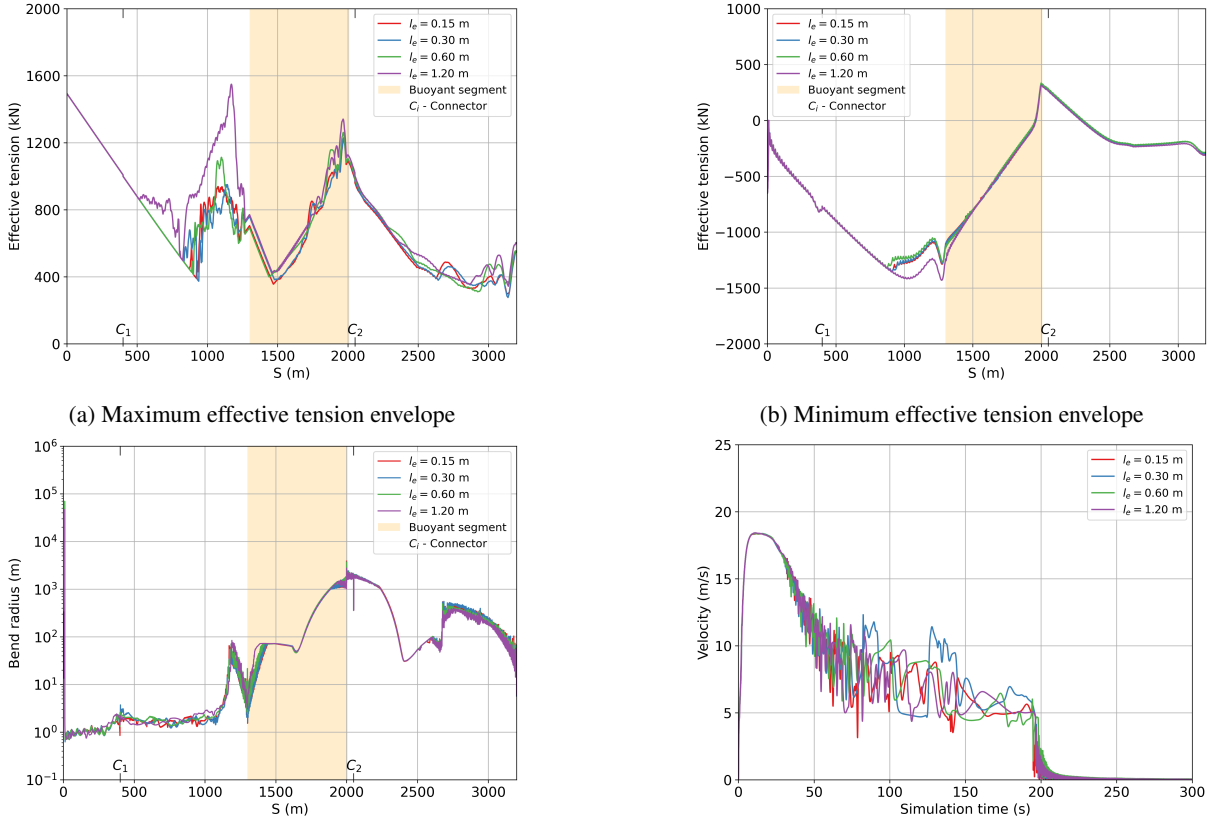
(d) Time step variation

Figure 4. Results for parametric study of the C_{Da}

Figure 4 shows how the envelopes for effective tension change for different C_{Da}. Using $C_{Da} = 0.002$, the model still exhibits a noisy response, which can also be seen by analyzing the time step variation, in Fig. 4d. For C_{Da} values above 0.004, envelopes for effective tension demonstrate similar behavior along nearly the entire riser length, except in the region immediately preceding the buoys, which shows greater variation in the effective tension. Figure 4d demonstrates that a low C_{Da} leads to significant time step variation and convergence difficulties. This behavior does not occur for axial drag coefficients above 0.004.

Regarding the first connector velocity, presented in Fig. 4c, the maximum values decrease with increasing axial drag coefficient. Overall, the presented results indicate that the model is highly sensitive to variations in the C_{Da}, especially regarding the body velocities.

Finally, the convergence study based on discretization is presented in Fig. 5. According to the results of the drag coefficient study, $C_{Da} = 0.006$ and C_{Dn} as a function of R_e were considered. The results show that for element lengths above the Euler limit ($l_e = 1.20$ m), the results are significantly affected. With $l_e \leq 0.60$ m, the maximum and minimum effective tensions exhibit similar behavior, indicating model convergence.



(a) Maximum effective tension envelope

(b) Minimum effective tension envelope

(c) Minimum bend radius envelope

(d) Velocity of the first connector (S = 400 m)

Figure 5. Results for different element lengths

As observed in Fig. 5d, regardless of mesh refinement, the maximum velocity magnitude converges to the same result: $v_{max} = 18.47$ m/s. This suggests that the maximum velocity at the first connector is relatively unaffected by discretization. An interesting aspect here is that, even though the problem is highly stochastic (as discussed in Meneses et al. [9]), this parameter seems to be more stable. Thus, it can be used for future model validation through field measurements during decommissioning. Regarding the minimum bend radius, shown in Fig. 5c, this parameter shows little sensitivity to discretization, as well as the other parameters studied in this work.

4 Final Remarks

It can be concluded that the computational model successfully produced consistent results and described the global behavior of the riser pull-out process when cut near the top end. The maximum time step study identified numerical noise when using insufficient time increments to represent the nonlinear dynamic behavior of the riser after cutting. The drag coefficient study demonstrated that adopting a conservative approach, valid for high Reynolds numbers where axial drag is neglected, is unfeasible due to convergence difficulties and significant nu-

merical noise. The axial drag coefficient was found to greatly influence the behavior of the riser during free-fall, reducing velocity and stabilizing the numerical response of the model. Conversely, the normal drag component showed minimal influence on the global pull-out behavior of the riser. Through convergence studies with element length reduction, the approach proposed by Meneses et al. [9] proved adequate for determining suitable element lengths for pull-out simulation. The chaotic behavior during free-fall requires particular attention, especially at locations with small bend radii. The maximum velocity was identified as a suitable model validation parameter due to its minimal sensitivity to the random nature of the phenomenon. Furthermore, the bend radius appears unaffected by the parameters studied, suggesting the need for additional research involving other parameters such as nonlinear moment-curvature relationships.

Finally, this work demonstrates the influence of key parameters for developing a concise numerical model. These results establish a foundation for future work incorporating non-deterministic studies and in-situ validation of free-fall behavior through field measurements.

Acknowledgements. The authors gratefully acknowledge Petrobras and CNPq (Conselho Nacional de Desenvolvimento Científico e Tecnológico) for the financial support.

Authorship statement. The authors hereby confirm that they are the sole liable persons responsible for the authorship of this work, and that all material that has been herein included as part of the present paper is either the property (and authorship) of the authors, or has the permission of the owners to be included here.

References

[1] ANP. Agencia nacional do petroleo, gas natural e biocombustiveis resolucao anp n 817. Technical report, Agencia Nacional do Petroleo, 2020.

[2] P. d. C. J. Vidal, M. O. A. González, de R. M. Vasconcelos, de D. C. Melo, de P. Oliveira Ferreira, P. G. V. Sampaio, and da D. R. Silva. Decommissioning of offshore oil and gas platforms: A systematic literature review of factors involved in the process. *Ocean engineering*, vol. 255, pp. 111428, 2022.

[3] N. S. Philip, S. Wilde, R. Arshad, I. Washash, and T. Al-Sayed. Decommissioning process for subsea pipelines. In *Abu Dhabi International Petroleum Exhibition and Conference*, pp. D021S035R005. SPE, 2014.

[4] A. Orr, S. Olmos, D. Cheek, M. Coyne, N. Tatineni, Y. Park, and D. Seal. Unconventional approach simplifies steel catenary riser decommissioning. In *Offshore Technology Conference*, pp. D041S052R005. OTC, 2021.

[5] A. C. Melilo Junior, Oliveira da C. H. Costa, C. A. Armani Delalibera, M. A. Schwingel Dias, Palmeira de T. M. Oliveira, and R. M. Pereira. Pre-laying of flexible lines flownline and riser and floaters in ultra deepwater. In *SPE Oil and Gas India Conference and Exhibition?*, pp. D031S017R003. SPE, 2019.

[6] M. Duan, J. Chen, K. Tian, and J. Zhang. A mechanical model for deepwater steel catenary riser transfer process during installation. *Proceedings of the Institution of Mechanical Engineers, Part M: Journal of Engineering for the Maritime Environment*, vol. 227, n. 1, pp. 3–11, 2013.

[7] M. Paredes, T. Wierzbicki, and C. C. Roth. Three dimensional, flexural-torsional dynamic buckling of long wires after tensile fracture and implications on deep water riser dynamics. *International Journal of Impact Engineering*, vol. 86, pp. 27–39, 2015.

[8] B. S. Matias, J. Aguiar Jr., E. Parente Jr., Cartaxo de A. M. Melo, and A. B. Custodio. Post-failure behavior of long wires under dynamic pulse buckling. *XLI Ibero-Latin American Congress on Computational Methods in Engineering*, vol. 2, n. 2, 2020.

[9] B. M. Meneses, L. G. Ribeiro, E. Parente, de A. M. C. Melo, da F. P. Silva Mineiro, and M. T. C. G. Carneseca. Post-failure behavior of lazy-wave risers. *Ocean Engineering*, vol. 280, pp. 114777, 2023.

[10] B. Meneses, R. Sousa, E. Parente, A. Melo, F. Mineiro, and M. Carneseca. Post-failure simulation of lazy-wave risers. *Proceedings of the XLI Ibero-Latin-American Congress on Computational Methods in Engineering*, vol. 41, pp. 1–7, 2020.

[11] L. G. Ribeiro, B. M. Meneses, J. Aguiar Jr, E. Parente Jr, de A. M. C. Melo, F. P. Mineiro, and M. T. Carneseca. Methodology for simulation of the post-failure behavior of flexible catenary risers. *Marine Structures*, vol. 82, pp. 103142, 2022.

[12] Orcina. Orcaflex user's manual.
`https://www.orcina.com/webhelp/OrcFxAPI/Default.htm`, acesso em 11/2024, 2024.

[13] D. Fergestad and S. A. Løtveit. Handbook on design and operation of flexible pipes, 2017.

[14] DNVGL-RP-C205. Environmental conditions and environmental loads, 2017.